

Experiment results of a novel sub-bottom profiler using synthetic aperture technique

Xuebo Zhang^{1,*}, Peixuan Yang¹ and Miao Sun²

¹Acoustic Signal and Electronics Science and Technology Corporation, Lanzhou 730050, China

²China Railway Twenty-one Bureau Group Corporation, Lanzhou 730000, China

Using Mills cross-configuration of multibeam sonar and synthetic aperture technique, a downward-looking synthetic aperture sonar (SAS), used for the sub-bottom profiler is presented here. The real data collected by the downward-looking SAS are processed by the multi-receiver SAS range migration algorithm. By analysing the performance of focused target, the buried object in the soft sediment layer below the seafloor can be well-reconstructed. Furthermore, it shows that the presented system has great potential in profiling the sediment layer below the seafloor.

Keywords: Cross configuration, imaging algorithm, multibeam sonar, synthetic aperture technique, sub-bottom profiler.

SINCE the signal with low frequency owns the characteristic of penetration in soft sediments, the sub-bottom profiler based on low frequency signal is commonly used to explore the sediment layer below the seafloor. Based on data collected from sub-bottom profilers, it is possible to characterize the morphology and sediment structures in the sub-bottom. The multibeam sub-bottom profiler, chirp sub-bottom profiler, parametric sub-bottom profiler and side-scan synthetic aperture sonar (SAS) profiler have been reported to detect sub-bottom sediments (Figure 1).

The multibeam sub-bottom profiler uses two large transducer arrays in a Mills cross-configuration¹ (Figure 1 a). It is T-shaped, in which both arrays have a special function. The transmitter array is mounted along the ship keel, while the receiver array is mounted perpendicular to the receiver array. Based on the beamforming technique, several beams corresponding to various reception angles can be generated. The chirp sub-bottom profiler is based on the linear frequency modulation (LFM) signal and mainly uses the pulse compression technique² (Figure 1 b). Both multibeam and chirp sub-bottom profilers belong to the real aperture sonar. Accordingly, the azimuth (along-track) resolution is determined by the real aperture. That is, the size of the sonar transducer must be very large if we must obtain high resolution. In Figure 1 c, two signals with slightly different primary high frequencies are transmitted by the parametric sub-bottom profiler^{3,4}. Based on the nonlinear property of underwater acoustic channel,

the difference between both transmitted frequencies generates a low frequency called the secondary frequency. The primary frequency is to measure the height, while the secondary frequency is to penetrate the sediment layer. Compared with the multibeam and chirp sub-bottom profilers at the same frequency, the size of the parametric sub-bottom profiler is small. However, the generation efficiency from primary to secondary wave is not efficient. Besides, the azimuth resolution is not focused by the parametric sub-bottom profiler. Currently, the side-scan SAS is employed to detect the sediment layer (Figure 1 d)^{5,6}. Using the synthetic aperture technique, a virtual array is created with the motion of a short transducer. Accordingly, the along-track resolution can be highly improved compared with the multibeam, chirp and parametric sub-bottom profilers. Generally speaking, the sediment penetration strongly depends on the energy of the transmitted signal. In other words, the side-scan SAS may fail to penetrate the seafloor sediment without sufficient signal energy, because some diffuse reflection of the echo signal cannot be received by the receiver. Using Mills cross-configuration of multibeam sonar and synthetic aperture technique of the SAS system, a downward-looking SAS used for the sub-bottom profiler is presented here. With this system, the contradiction between sediment penetration and signal energy can be resolved. Figure 2 shows the three-dimensional imaging geometry of the downward-looking SAS. The SAS system moves in a straight line along the y -axis and its velocity is v . The height of the sonar system is represented as r . The $y-z$ plane is the two-dimensional imaging geometry. On the one hand, the receiver and transmitter arrays are configured with Mills cross-configuration, which is used by the multibeam sonar. In the presented SAS system, the receiver array is mounted along the ship keel while the transmitter array is mounted perpendicular to the receiver array. It can be clearly seen that the array deployment of the system is directly opposite to

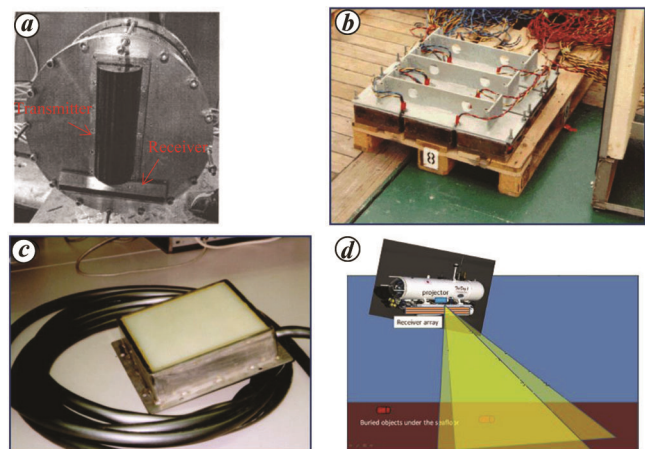


Figure 1. Sub-bottom profilers: **a**, multibeam profiler; **b**, chirp profiler; **c**, parametric profiler; **d**, side-scan synthetic aperture sonar (SAS) profiler.

*For correspondence. (e-mail: xuebo_zhang@sina.cn)

that of the multibeam sonar. On the other hand, the sonar looks downwards at the flight path. Therefore, the sediment layer can strongly reflect the energy in the incoming direction at normal incidence. This is the major difference between the downward-looking SAS and side-scan SAS. Furthermore, the presented system concentrates on the narrow swath imaging compared with the side-scan SAS system. This would be helpful for sediment penetration.

Since the presented system is based on the sediment penetration of low-frequency signals, the medium refraction index of the sediment layer below the seafloor would affect the processing performance. For simplicity, the medium refraction index is not considered in this study as the effectiveness of the presented system is the main focus of attention. This system would also suffer from motion errors like traditional SAS systems. In general, large motion errors can be obtained based on the inertial navigation system such as Doppler velocity log, global positioning system, ultra-short baseline and sound velocity profile. The small motion errors can be estimated from the echo data. With the known motion error, the motion compensation algorithms are employed before the synthetic aperture image formation⁷. Generally, motion error which is larger than quarter wavelength should be considered. Since the presented system works with low frequency, the motion error slightly affects the imaging performance. Due to these reasons, the motion error is not taken into account in order to simplify the signal processor. The collected data can be processed based on the multireceiver SAS imaging algorithms, such as range migration algorithm⁸ and back projection algorithm⁹. Figure 3 presents the real SAS system. Both transmitter and receiver arrays include eight elements and the diameter of each element is 0.08 m. The chirp signal is used as the transmitted signal, which has a 7 kHz bandwidth at a centre frequency of 12 kHz. The pulse repetition interval is 0.06 s. The sonar is towed with 2 m/s.

Before the SAS imagery, the echo data corresponding to two adjacent receivers are superposed. After this processing, the diameter of each element changes to 0.16 m. The multireceiver SAS range migration algorithm including two important steps is used to process the data. The first step is to perform the preprocessing, which coerces the multireceiver SAS signal into monostatic SAS equivalent data based on the phase centre approximation (PCA) method¹⁰. Using the PCA method, the bistatic sonar can be considered to be a monostatic sonar located at the midpoint between the transmitter and receiver. However, this operation would introduce the approximation error called PCA error. Besides, the spatial data sampled by each receiver are highly undersampled, and do not satisfy the Nyquist sampling theorem. In general, each receiver is sampled at the $(1/M)$ th full sampling rate in the azimuth dimension based on the multiple channel sampling theorem. Here, M denotes the total number of receivers. Thus,

the preprocessing mainly carries out two tasks¹⁰. One is to compensate the PCA error and the other is to recover the azimuth spectrum satisfying full sampling rate. After carrying out the preprocessing¹⁰, the second step is the synthetic aperture image formation using range migration algorithm designed for a monostatic SAS system⁸. Figure 4 shows the block diagram for data processing.

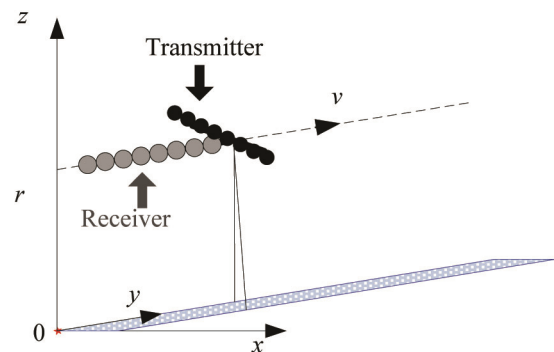


Figure 2. Imaging geometry of downward-looking SAS.



Figure 3. Real system of downward-looking SAS.

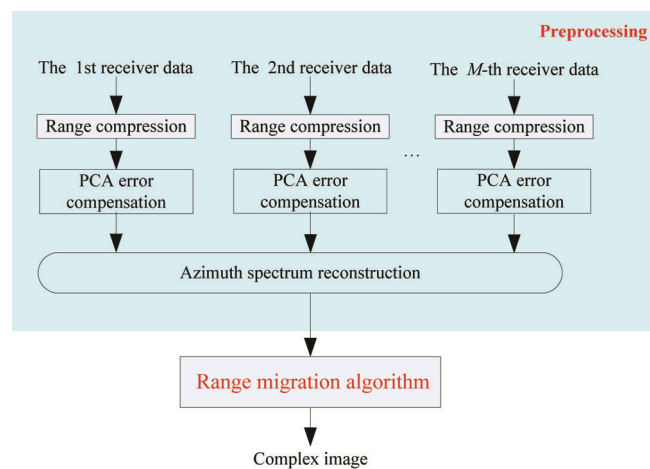


Figure 4. Block diagram of the presented method.

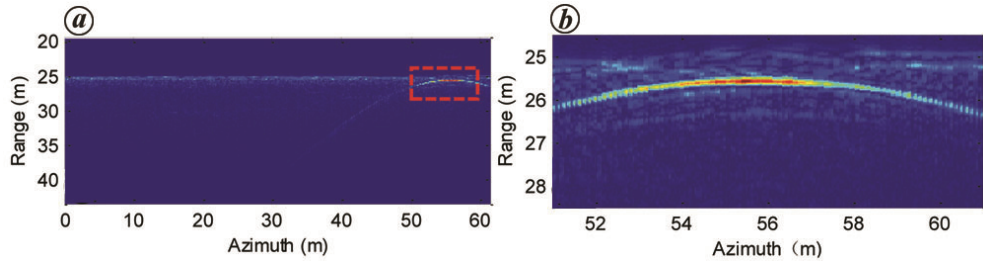


Figure 5. Signal after preprocessing. *a*, Data after range compression. *b*, Zoomed-in view of the target.

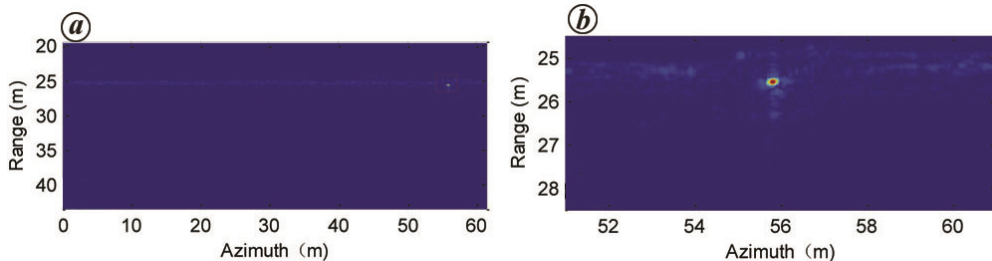


Figure 6. Focusing result. *a*, Imaging result. *b*, Zoomed-in view of the target.

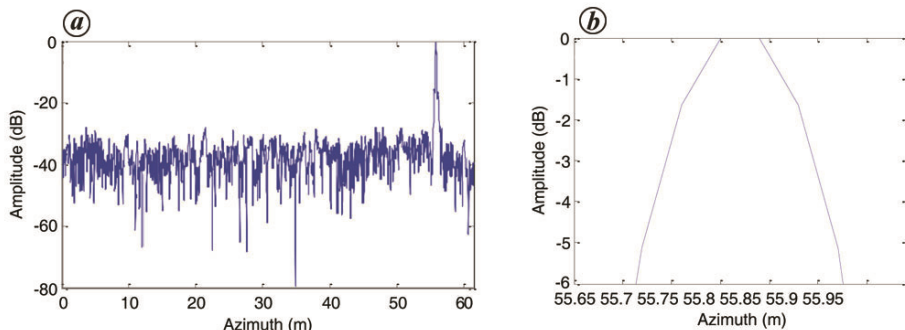


Figure 7. Azimuth slice of the focused target. *a*, Azimuth slice. *b*, Zoomed-in view of the azimuth slice.

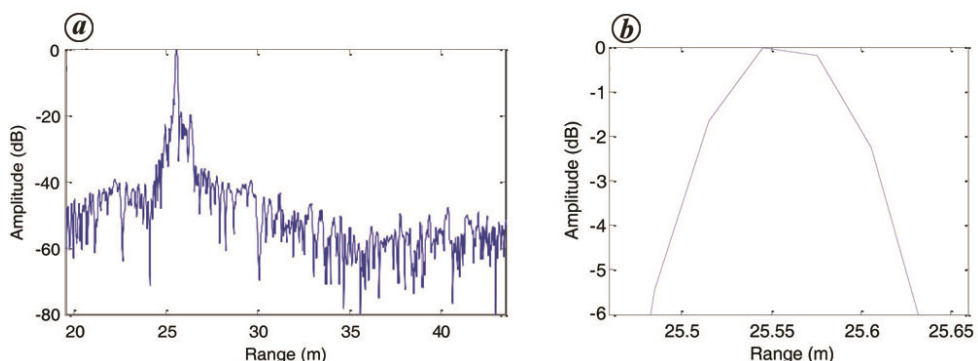


Figure 8. Range slice of the focused target. *a*, Range slice. *b*, Zoomed-in view of the range slice.

Figure 5 *a* shows the results after preprocessing the echo data. Figure 5 *b* shows the zoomed – in view of the target corresponding to the red dashed area in Figure 5 *a*. It can be found from Figure 5 that there is a strong reflectivity target in the sediment layer below the seafloor.

Generally, the penetration reaches a few tens of decimetres in soft sediments.

The data shown in Figure 5 *a* are considered to be the input of the range migration algorithm designed for monostatic SAS system⁸. Figure 6 *a* depicts the focusing

result. Figure 6 *b* shows the zoomed-in view of the target corresponding to the red dashed area in Figure 6 *a*. It can be clearly observed that the target in the sediment layer is well-reconstructed. This means that the presented system can be used for the sub-bottom profiler.

In order to visually evaluate the imaging performance, the azimuth and range slices were analysed in detail. Figure 7 *a* shows the azimuth slice. Figure 7 *b* shows the zoomed-in view of the azimuth slice. Figure 7 *b*, the azimuth resolution is about 0.15 m, which is not equal to the theoretical resolution of 0.08 m. In general, the synthetic aperture technique can theoretically promise high resolution of 0.08 m. In practice, it is always difficult to achieve full theoretical resolution, because the SAS system suffers from motion error, multipath in shallow water, and so on. Considering these factors, a simple rule of thumb is that the practical resolution would be 1.5–2 times lower¹¹. At this point, the resolution shown in Figure 7 *b* is approximately close to the theoretical resolution.

Figure 8 *a* depicts the range slice and Figure 8 *b* shows the zoomed-in view of the range slice. The theoretical resolution in the vertical dimension is directly determined by the signal bandwidth and it is 0.11 m. From Figure 8 *b*, the vertical resolution is about 0.12 m. This means that the vertical resolution shown agrees well with the theoretical resolution.

Based on the processing results of real data, we conclude that the downward-looking SAS with Mills cross configuration can obtain high-resolution image of the sediment layer. It can also be used for the exploration of buried objects in the sediment layer. Some buried objects such as mines and chemical ammunition are hazardous. With the presented system, these objects can be efficiently detected and cleared. It can also be used to detect buried relics by the archaeologists and has great potential in exploring the sediment layer below the seafloor. Using this system, the morphology and sediment structures in the sub-bottom such as steep slopes, faults, reefs, landslide areas, ridges and rocky outcrops can be characterized. The results can be used for underwater engineering such as pipeline deployment, mineral resources investigations, bridge-building, shore protection and waterway dredging.

1. Ramsay, P. and Miller, W., Multibeam and sub-bottom profiling surveys for major port expansions. *Position IT*, 2010, 29–33.
2. Gutowski, M., Bull, J., Henstock, T., Dix, J., Hogarth, P., Leighton, T. and White, P., Chirp sub-bottom profiler source signature design and field testing. *Mar. Geophys. Res.*, 2002, **23**, 481–492.
3. Qu, K., Zou, B., Chen, J., Guo, Y. and Wang, R., Experimental study of a broadband parametric acoustic array for sub-bottom profiling in shallow water. *Shock Vib.*, 2018; doi:10.1155/2018/3619257.
4. Saleh, M. and Rabah, M., Seabed sub-bottom sediment classification using parametric sub-bottom profiler. *NRIAG J. Astron. Geophys.*, 2016, **5**, 87–95.
5. Asada, A., Ura, T., Maeda, F., Maki, T., Yamagata, Y. and Seiichi, T., Sub-bottom synthetic aperture imaging sonar system using an AUV and an autonomous surface tracking vehicle for searching

for buried shells of toxic chemicals. In Proceedings – International Waterside Security Conference, Carrara, Italy, 2010, doi:10.1109/WSSC.2010.5730223.

6. Varghese, S. et al., Synthetic aperture sonar image of seafloor. *Curr. Sci.*, 2017, **113**, 385.
7. Wang, G., Zhang, L., Li, J. and Hu, Q., Precise aperture-dependent motion compensation for high-resolution synthetic aperture radar imaging. *IET Radar Sonar Navig.*, 2017, **11**, 204–211.
8. Zhang, X., Tang, J., Zhong, H. and Zhang, S., Wavenumber-domain imaging algorithm for wide-beam multi-receiver synthetic aperture sonar. *J. Harbin Eng. Univ.*, 2014, **35**, 93–101.
9. Zhang, X., Yang, P., Tan, C. and Ying, W., BP algorithm for the multireceiver SAS. *IET Radar Sonar Navig.*, 2019, **13**, 830–838.
10. Zhang, X., Tang, J. and Zhong, H., Multireceiver correction for the chirp scaling algorithm in synthetic aperture sonar. *IEEE J. Ocean. Eng.*, 2014, **39**, 472–481.
11. Hagen, P. and Hansen, R., Area coverage rate of synthetic aperture sonars. In Proceedings – Europe Oceans, Aberdeen, UK, 2007; doi:10.1109/OCEANSE.2007.4302382.

ACKNOWLEDGEMENTS. We thank the National Natural Science Foundation of China and the National Key Laboratory Foundation, China for support. We also thank the anonymous reviewers for useful suggestions that helped improve the manuscript.

Received 25 November 2019; revised accepted 11 January 2022

doi: 10.18520/cs/v122/i4/461-464

Efficient molecular method/s for detection of *Bt* brinjal Event 142

Ruchi Sharma, Monika Singh and Gurinderjit Randhawa*

Division of Genomic Resources, ICAR-National Bureau of Plant Genetic Resources, New Delhi 110 012, India

Fruit and shoot borer (FSB)-resistant *Bt* brinjal Event 142 with *cry1Fa1* gene has been approved for biosafety research level (BRL)-II field trials by the Genetic Engineering Appraisal Committee (GEAC), the competent authority in India. For regulatory compliance, systematic detection of genetically modified (GM) crops would facilitate monitoring for the presence of a GM event in the supply chain. Polymerase chain reaction (PCR) and real-time PCR are widely used for GM detection globally. Qualitative PCR and real-time PCR assays targeting *cry1Fa1* transgene were developed and validated with acceptable specificity and sensitivity up to 0.01%. A multiplex (hexaplex) PCR-based screening assay simultaneously detecting five transgenic elements and an endogenous gene was developed for Event 142. Construct-specific PCR reported herein could be employed for more specific

*For correspondence. (e-mail: gurinder.randhawa@icar.gov.in)